## Cume #417

63 Points Possible; 45 Points is Guaranteed Pass passes below this score are a distinct possibility Administered September 16, 2017

Discovery of an HI-Rich Gas Reservoir in the Outskirts of SZ-Effect Selected Clusters Sowgat Muzahid, Jane Charlton, Dansuke Nagai, Joop Schaye, & Raghunathan Srianand arXiv:1708.02600v1 (August 8, 2017)

You may use a calculator, but no programmed formulae. Some physical constants are supplied in the exam as needed. Please start each question (by number) on a new sheet of paper, write on only one side of the paper, and staple them together in order of question number when finished. Please present your results in the order that the individual questions appear and clearly label each problem number. Keep away from the upper left corner of your paper - do not obscure your work or the problem number underneath the staple!

- 1. [12 pts] Write a very brief overview of this paper. Be sure you emphasize the central <u>scientific</u> point or points (i.e., what is the big picture the authors attempted to demonstrate to the reader). Clearly separate your responses into the following well-defined categories—I am testing that you can properly delineate the author's motivations, methods, analysis, and results.
  - (a) [3 pts] In three sentences maximum, describe the big picture broader astronomical context motivating this work.
  - (b) [3 pts] In three sentences maximum, describe the data employed, observations, and observational methods. (do not describe analysis or results here)
  - (c) [3 pts] In three sentences maximum, describe scientific analysis performed (do not describe results or findings here).
  - (d) [3 pts] In three sentences maximum, describe the new most important conclusion(s) [those central to the larger picture addressed by the paper, i.e., your "walk away" results].
- 2. [18 pts] Measuring the H<sub>I</sub> column density. In Figure 1, the authors display the background quasar spectra with the neutral hydrogen absorption indicated. They state that the spectra are "showing the Lyman limit breaks caused by the absorbers."
  - (a) [4 pt] What physical process creates the Lyman limit break feature in the spectra? Provide which element/ion it arises from and the physics of the process at the atomic level. What is the wavelength of the Lyman break in the rest-frame of the gas?
  - (b) [4 pt] Consider the spectrum of the quasar J0040-5057 in Figure 1. Given the precise absorption redshift of  $z_{\rm abs} = 0.43737$  measured from the many bound-bound absorption lines from the CCM HI gas (pink tick marks). At what wavelength would the Lyman limit break be predicted in the spectrum? Is yur answer consistent with the spectrum in Figure 1? Explain.
  - (c) [10 pt] From the spectrum of the quasar J2109-5042 in Figure 1, and using the authors estimated continuum value blueward of the Lyman break,  $F_{\lambda}^{-}$ , and estimated continuum value redward of the break,  $F_{\lambda}^{+}$ , compute the H<sub>I</sub> column density, N(HI), from the observed Lyman limit break. HINT: Use the radiative transfer solution  $F_{\lambda}^{-}/F_{\lambda}^{+} = \exp(-\tau_{\lambda})$  and the definition of optical depth  $\tau_{\lambda} = \int n\sigma_{\lambda}ds = N\sigma_{\lambda}$ , where  $\sigma_{\lambda} = 6.03 \times 10^{-18} \text{ cm}^2$  is the cross section for absorption at the Lyman limit. (check your value with the author's value!)
- 3. [15 pts] Near the beginning of the discussion section, the authors "compute the probabilities of random occurrence of each absorber around the cluster redshift within the  $\pm 1~\sigma$  of the cluster redshifts by using the observed  $d\mathcal{N}(>N)/dz$  of low-z H<sub>I</sub> absorbers" from Danforth et al. (2016).
  - (a) [3 pt] What are the authors attempting to demonstrate by making this calculation and why is it astrophysically important?
  - (b) [4 pt] The quantity  $d\mathcal{N}/dz$  is often referred to as the "redshift path density". In your own words, what does "redshift path density" actually measure (the definition is not in the paper). What does the argument (>N) in  $d\mathcal{N}(>N)/dz$  mean?

- (c) [8 pt] Let's say you conduct a survey for HI absorption lines in a sample of spectra that probe the universe from z=2.3 to z=0.6 and you find the results provided in Table 1 (of this exam). Use these data to compute  $d\mathcal{N}(>N)/dz$  for  $N=10^{15}$  cm<sup>-2</sup> for your survey.
- 4. [18 pts] The authors compute a probability of random occurrence of 8.7% for the z = 0.51 absorber toward J2109-5042. They certainly do not show how they make this computation, leaving it as an excercise for the reader! So, we want to reproduce their result.
  - (a) [6 pt] Simplifying the problem by assuming a uniform redshift distribution for H<sub>I</sub> absorbers along a line of sight, show that the probability for random occurrence in a redshift interval  $\Delta z$  can be written  $P = \Delta z/[dN(>N)/dz]^{-1} = [dN(>N)/dz] \cdot \Delta z$ . By "show" I am looking not only for algebraic manipulation of mathematical expressions, but for text that describes and explains how you arrive at the final expression. A diagram may be helpful.
  - (b) [4 pt] In §3, the authors make the statement "This absorber shows a somewhat larger systemic velocity of  $\simeq +9000$  km s<sup>-1</sup> with respect to the cluster J2109–5040." The  $\Delta z$  in our equation for P is the redshift path between the absorbing gas that gives rise to the Lyman break and the cluster. What is the value of  $\Delta z$ .
  - (c) [4 pt] Looking up Danforth's paper, you find that he provides the following fit for

$$\frac{dN(>N)}{dz} = 16(1+z)^{2.3} \left(\frac{N}{10^{14}}\right)^{(0.31z-0.75)}.$$
 (1)

Use this fit result to compute  $d\mathcal{N}(>N)/dz$  for this system.

(d) [4 pt] Now use the equation for P from part (a) and compute the probability of incidence within  $\pm 1$   $\sigma$  of the cluster redshift. Did you obtain a result consistent with that of the author's?

TABLE 1 HI ABSORBERS

QSO	redshift	$\log N({\rm H{\sc i}})~{ m cm}^{-2}$	QSO redshift $\log N({\rm HI})~{\rm cm}^{-2}$
J0000-123	0.609	14.20	J1038+459 0.894 13.22
J0000-123	1.980	14.35	J1038#459 1.712 13.86
J0000-123	2.170	15.80	J1038+459 sen1.836 cas 1 16.38
J0345+051	0.711	14.98	J1038+459 1.849 13.98
J0345+051	1.017	13.67	J1038+459 2.001 14.15
J0345+051	1.111	13.96	J1317+109 1.203 13.55
J0345+051	1.924	14.02	J1317+109 1.344 14.74
J0345 + 051	2.209	17.90	J1317+109 1.833 13.22
J0450+710	0.873	13.87	J1623+378 0.778 14.00
J0450+710	0.998	14.66	J1623+378 1.099 14.86
J0450+710	1.567	13.21	J1623+378 1.345 12.90
J0831 - 217	1.145	13.77	J1623+378 1.876 13.72
J0831 - 217	1.690	14.20	J2022-001 0.750 19.03
J0831 - 217	1.864	13.37	J2022-001 2.210 14.45
J0831-217	2.225	14.31	

# DISCOVERY OF AN HI-RICH GAS RESERVOIR IN THE OUTSKIRTS OF SZ-EFFECT SELECTED CLUSTERS

SOWGAT MUZAHID<sup>1</sup>, JANE CHARLTON<sup>2</sup>, DAISUKE NAGAI<sup>3</sup>, JOOP SCHAYE<sup>1</sup>, AND RAGHUNATHAN SRIANAND<sup>4</sup>

<sup>1</sup>Leiden Observatory, Leiden University, PO Box 9513, NL-2300 RA Leiden, The Netherlands (sowgat@strw.leidenuniv.nl)
<sup>2</sup>Department of Astronomy & Astrophysics, The Pennsylvania State University, State College, PA 16801, USA
<sup>3</sup>Department of Physics, Yale University, New Haven, CT 06520, USA
<sup>4</sup>Inter-University Centre for Astronomy and Astrophysics, Post Bag 4, Ganeshkhind, Pune 411 007, India

Draft version August 10, 2017

### **ABSTRACT**

We report on the detection of three strong H I absorbers originating in the outskirts (i.e., impact parameter,  $\rho_{\rm cl} \approx (1.6$ –4.7) $r_{500}$ ) of three massive ( $M_{500} \sim 3 \times 10^{14}~M_{\odot}$ ) clusters of galaxies at redshift  $z_{\rm cl} \approx 0.46$ , in the Hubble Space Telescope Cosmic Origins Spectrograph (HST/COS) spectra of 3 background UV-bright quasars. These clusters were discovered by the 2500 deg² South Pole Telescope Sunyaev–Zel'dovich (SZ) effect survey. All three COS spectra show partial Lyman limit absorber with  $N({\rm H\,I}) > 10^{16.5}~{\rm cm}^{-2}$  near the photometric redshifts ( $|\Delta z/(1+z)|\approx 0.03$ ) of the clusters. The compound probability of random occurrence of all three absorbers is < 0.02%, indicating that the absorbers are most likely related to the targeted clusters. We find that the outskirts of these SZ-selected clusters are remarkably rich in cool gas compared to existing observations of other clusters in the literature. The effective Doppler parameters of the Lyman series lines, obtained using single cloud curve-of-growth (COG) analysis, suggest a non-thermal/turbulent velocity of a few×10 km s<sup>-1</sup> in the absorbing gas. We emphasize the need for uniform galaxy surveys around these fields and for more UV observations of QSO-cluster pairs in general in order to improve the statistics and gain further insights into the unexplored territory of the largest collapsed cosmic structures.

Keywords: galaxies: clusters: intracluster medium — galaxies: halos — quasars: absorption lines — intergalactic medium

## 1. INTRODUCTION

Galaxy clusters are the most massive gravitationally bound structures in the universe. With 100–1000 galaxies and total masses of  $\sim \! 10^{14-15}~M_{\odot}$ , gas accreting onto a cluster is typically heated to a very high temperature. In fact, X-ray observations have revealed enormous quantities of diffuse, hot ( $\sim \! 10^{7-8}~\rm K$ ) gas in the central regions of galaxy clusters within which the mean mass density is over 500 times the critical density of the universe (i.e.,  $< r_{500}$ ; see Voit (2005), for a review). The origin of the energy radiated away via X-rays, which have been the main source of information on the ICM so far, is thermal bremsstrahlung with power,  $P \propto n_e^2 T_e^{1/2}$ . However, the ICM in cluster outskirts (i.e.,  $\rho_{\rm cl} \sim (1-5)r_{500}$ ), where the density and temperature are considerably lower than in the core, is not bright enough to detect in X-ray emission. Consequently, the outskirts of galaxy clusters, particularly at high-z, are not well explored observationally. This is partly because of the lack of sensitive diagnostics for probing the cool/warm-hot gas, with  $T \sim \! 10^{4-6}~\rm K$ , that prevails in the circumcluster medium (CCM).

In recent years, with the advent of high resolution cosmological simulations and deep X-ray observations of a handful of nearby clusters, cluster outskirts have emerged as one of the new frontiers of study in cluster astrophysics and cosmology (e.g., Simionescu et al. 2011; Walker et al. 2012; Urban et al. 2014; Lau et al. 2015; Bahé et al. 2017). This environment is the interface between clusters and the cosmic web. In the outskirts, galaxies and groups of galaxies are stripped of their metal-rich gas by tidal forces and by the ram pressure provided by the cluster, enriching the ICM with heavy elements. The outskirts of galaxy clusters may harbor a substantial fraction of the "missing baryons" (e.g., Gonzalez et al. 2007,

2013) which could reside in the cool/warm-hot ( $T \sim 10^{4-6}$  K) gas phase. Probing the CCM is thus crucial for understanding gas flows, metal enrichment history, and the baryon budget in the largest collapsed environments.

Since cluster outskirts are beyond the reach of present day X-ray telescopes, an effective alternative is to use absorption line spectroscopy of background UV-bright quasars to probe the CCM. This technique has provided a wealth of information regarding the circumgalactic medium (CGM) of both low- and high-z galaxies (e.g., Turner et al. 2014; Werk et al. 2014; Kacprzak et al. 2015). However, except for a very few studies (i.e., Yoon et al. 2012; Yoon & Putman 2017; Burchett et al. 2017), it has not yet been used to probe the CCM. Yoon et al. (2012) have studied 43 Ly\alpha absorbers along 23 background QSO-sightlines towards the Virgo cluster using COS, STIS, and GHRS data. Interestingly, they found that the cool gas in Virgo is preferentially located in the cluster outskirts and is associated with substructures. Recently, Burchett et al. (2017) have studied the CCM of 7 X-ray detected clusters with masses of  $M_{200} \sim \text{few} \times 10^{14} M_{\odot}$ . Their sightlines typically pass within 300 kpc of a cluster galaxy. They have reported a very low covering fraction (≈ 18%) of H1 absorbing gas (equivalent width > 30 mÅ) in the CGM of cluster galaxies as compared to field/group galaxies ( $\approx 80-100\%$ ).

Motivated by the lack of UV observations of the CCM and its importance, we have built a sample of QSO-cluster pairs by cross-correlating the SZ-effect selected cluster catalog of Bleem et al. (2015) and the all-sky UV-bright QSO catalog (UVQS) of Monroe et al. (2016). As a pilot program we have obtained far-UV (FUV) spectra of 3 quasars using HST/COS. These quasars probe the outskirts of 3 SZ-selected clusters of masses  $M_{500} \sim 3 \times 10^{14}~M_{\odot}$  at red-

Table 1
Details of the QSO-cluster pairs

Cluster	RA <sub>c1</sub> (J2000)	DEC <sub>cl</sub> (J2000)	$z_{ m cl}$	$M_{500} (10^{14} M_{\odot})$	r <sub>500</sub> (Mpc)	QSO	$z_{ m qso}$	FUV	ρ <sub>cl</sub> (Mpc)	$ ho_{ m cl}/r_{ m 500}$	$z_{ m abs}$	$\frac{\log N(\text{H I})}{(N/\text{cm}^{-2})}$
(1)	(2)	(3)	(4)	(5)	(6)	(7)	(8)	(9)	(10)	(11)	(12)	(13)
J0041-5107 J2016-4517 J2109-5040	10.2932 304.0050 317.3825	-51.1286 -45.2978 -50.6765	$0.45 \pm 0.04$ $0.45 \pm 0.03$ $0.47 \pm 0.04$	3.04±0.87 3.19±0.89 3.81±0.87	0.87 0.89 0.93	J0040-5057 J2017-4516 J2109-5042	0.608 0.692	17.43 17.81 17.93	3.80 4.20 1.47	4.4 4.7 1.6	0.43737 0.43968 0.51484	$18.63 \pm 0.07$ $16.52 \pm 0.05$ $16.68 \pm 0.03$

Notes—Cluster's name (column 1), right ascension (column 2), declination (column 3), photometric redshift (column 4), and mass (column 5) are from Bleem et al. (2015). The  $r_{500}$  values are listed in column 6. QSO's name (column 7), emission redshift (column 8), and FUV magnitude (column 9) are from Monroe et al. (2016). The impact parameters and normalized impact parameters of the QSO sightlines are listed in columns 10 & 11, respectively. The absorption redshifts and the H1 column densities measured from COS data are listed in columns 12 & 13, respectively. The N(H1) values are obtained using single cloud COG analysis of Lyman series lines. These values are consistent with the ones obtained from the Lyman limit breaks. We note that the errors in the column densities are underestimated since we do not take the continuum placement uncertainties into account. A more realistic error would be 0.10-0.15 dex.

shift  $z_{\rm cl}\approx 0.46$  with impact parameters,  $\rho_{\rm cl}$ , of 1.5–4.2 Mpc  $(\rho_{\rm cl}/r_{500}\approx 1.6$ –4.7). The details of the QSO-cluster pairs are listed in Table 1. Intriguingly, in all three cases we detect strong H I absorption with  $N({\rm H\,I})>10^{16.5}~{\rm cm}^{-2}$  at the redshifts of the foreground clusters.

This Letter is organized as follows: In Section 2 we describe our COS observations. The analysis and the main results are presented in Section 3. The possible implications of our observations are discussed in Section 4. Throughout the Letter we adopt a flat  $\Lambda$ CDM cosmology with  $H_0 = 71 \text{ km s}^{-1} \text{ Mpc}^{-1}$ ,  $\Omega_{\rm M} = 0.3$ , and  $\Omega_{\Lambda} = 0.7$ . All the distances given are proper (physical) distances.

#### 2. OBSERVATIONS

UV spectra of the three background UV-bright (FUV < 18) quasars were obtained using HST/COS Cycle-24 observations under program ID: GO-14655 (PI: Muzahid). The properties of COS and its in-flight operations are discussed in Osterman et al. (2011) and Green et al. (2012). The observations consist of G130M and G160M FUV grating integrations covering 1100-1800 Å at a medium resolution of  $R \sim 18,000^{1}$ . The data were retrieved from the HST archive and reduced using the STScI CalCOS v3.1.8 pipeline software. The reduced, flux calibrated individual exposures were aligned and coadded using the IDL code "coadd\_x1d"(v3.1) developed by Danforth et al. (2010). The combined spectra have a signal-to-noise ratio (S/N) of 5-10 per resolution element. Each combined spectrum was binned by 3 pixels since the COS FUV spectra, with six raw pixels per resolution element, are highly oversampled. The analysis/results presented here are not affected by this re-binning. Continuum normalizations were done by fitting the line-free regions with smooth low-order polynomials.

## 3. ANALYSIS & RESULTS

In this section, we will first describe the properties of the absorbers and the targeted clusters. Next, the newly obtained data will be compared with those in the literature.

1. The  $z_{\rm abs}=0.43737$  system towards UVQSJ0040-5057: The absorber has a systemic velocity of  $\approx -2600~{\rm km~s^{-1}}$  with respect to the photometric-redshift (0.45 $\pm$ 0.04) of the cluster J0041-5107 (Bleem et al. 2015). This velocity is well within the  $1\sigma$  uncertainty of the cluster redshift, i.e.,  $|\Delta z/(1+z)| \approx 0.03 \approx 9000~{\rm km~s^{-1}}$ . This is the

strongest H I absorber among the three systems studied here, producing a full H I Lyman limit break at  $\approx 1315$  Å (see the top panel of Fig. 1). The full break allows us to estimate a lower limit on  $N({\rm H\,I})^2$  of  $10^{17.7}$  cm $^{-2}$  assuming the flux below 1315 Å to be less than  $10^{-16}$  erg cm $^{-2}$  s $^{-1}$  Å $^{-1}$ . A single component curve-of-growth (COG) analysis of all the unblended Lyman series lines yields a column density of  $10^{18.63\pm0.07}$  cm $^{-2}$  and an effective Doppler parameter of  $b_{\rm eff}=41\pm1$  km s $^{-1}$  (see Fig. 2). The mass of the corresponding cluster is  $M_{500}=(3.04\pm0.87)\times10^{14}~M_{\odot}$ , corresponding to  $r_{500}=0.87$  Mpc (see Table 1). The impact parameter of 3.80 Mpc gives  $\rho_{\rm cl}/r_{500}\approx4.4$ .

2. The  $z_{\rm abs}=0.43968$  system towards UVQSJ2017–4516: The systemic velocity of the absorber with respect to the photometric redshift of the corresponding cluster (J2016–4517) is  $\approx -2100~{\rm km~s^{-1}}$ , which is well within the  $1\sigma$  uncertainty ( $|\Delta z/(1+z)| \approx 0.02 \approx 6000~{\rm km~s^{-1}}$ ) of the cluster's photometric redshift (Bleem et al. 2015). The absorber exhibits a partial break at the H I Lyman limit corresponding to  $N({\rm H\,I}) \approx 10^{16.6}~{\rm cm^{-2}}$  (see middle panel of Fig. 1). A single component COG analysis of all the unblended Lyman series lines gives a consistent  $N({\rm H\,I})$  of  $10^{16.52\pm0.05}~{\rm cm^{-2}}$  and  $b_{\rm eff}$  of  $25\pm1~{\rm km~s^{-1}}$  (see Fig. 2). The mass and radius of the cluster are  $M_{500}=(3.19\pm0.89)\times10^{14}~M_{\odot}$  and  $r_{500}=0.89~{\rm Mpc}$ , respectively. The impact parameter of 4.20 Mpc corresponds to  $\rho_{\rm cl}/r_{500}\approx4.7$ .

3. The  $z_{\rm abs}=0.51484$  system towards UVQSJ2109–5042: This absorber shows a somewhat larger systemic velocity of  $\approx +9000~{\rm km~s^{-1}}$  with respect to the cluster J2109–5040. Such a velocity, however, is consistent within the  $1\sigma$  uncertainty of the cluster's photometric redshift, i.e.,  $|\Delta z/(1+z)| \approx 0.03 \approx 9000~{\rm km~s^{-1}}$  (Bleem et al. 2015). The partial break seen in the COS spectrum (see the bottom panel of Fig. I) gives  $N({\rm H~I}) \approx 10^{16.8}~{\rm cm^{-2}}$  which is consistent with the value we obtain from COG analysis of the unblended Lyman series lines (i.e.,  $10^{16.68\pm0.03}~{\rm cm^{-2}}$ , see Fig. 2). We obtain  $b_{\rm eff}$  of  $32\pm1~{\rm km~s^{-1}}$  from the COG analysis. The mass of the cluster,  $M_{500}=(3.81\pm0.87)\times10^{14}~M_{\odot}$ , corresponds to  $r_{500}=0.93~{\rm Mpc}$ . The impact parameter of the cluster of 1.5 Mpc so that  $\rho_{\rm cl}/r_{500}\approx1.6$ .

In Fig. 3 we show the clustocentric radial profile of  $N({\rm H\,I})$ , combining our measurements with the handful of studies that exist in the literature. The data points corresponding to the Virgo and Coma clusters are taken from Yoon et al. (2012) and

 $<sup>^{1}</sup>$  No flux is observed below 1315 Å in the spectrum of QSO UVQS J0040–5057 due to the strong Lyman limit break in the spectrum caused by the  $z_{\rm abs}=0.43737$  absorber studied here.

 $<sup>^2</sup>$   $N({\rm H\,I})=\frac{\tau_{\rm LL}}{\sigma_{\rm H\,I}}$ ; where  $\sigma_{\rm H\,I}\approx 6.3\times 10^{-18}~{\rm cm^2}$  is the H I photoionization cross-section and  $\tau_{\rm LL}=-\ln(\frac{I}{I_0})$  is the optical depth at the Lyman limit.

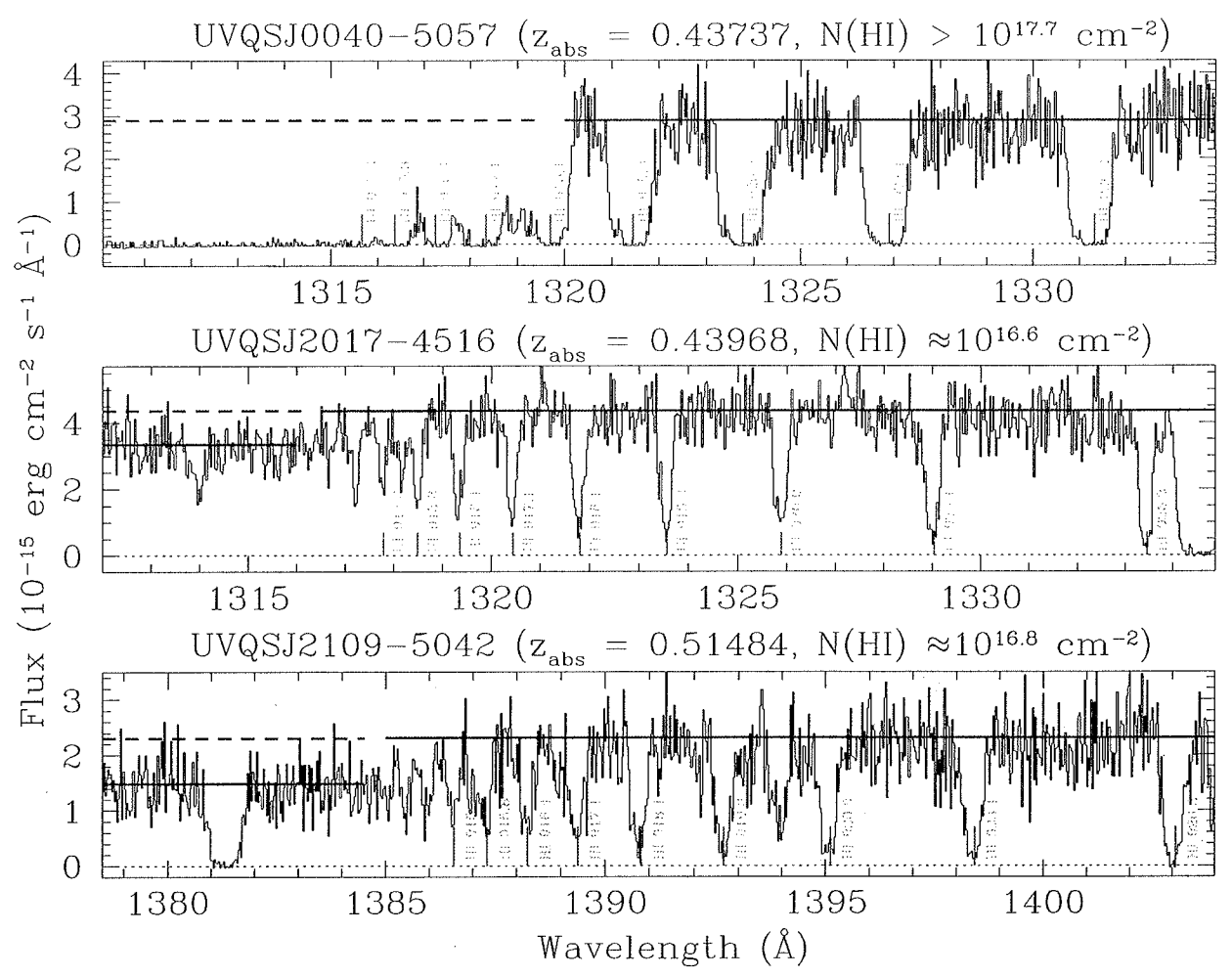


Figure 1. Selected parts of the COS spectra showing the Lyman limit breaks caused by the absorbers with redshifts consistent with the photometric redshifts of the targeted clusters. The higher order H I Lyman series lines are marked. The horizontal (red) lines are the adopted continua. The horizontal (blue) dashed lines bluewards the Lyman limit breaks are the extrapolated continua. The full break produced by the absorber at  $z_{abs} = 0.43737$  towards UVQS J0040–5057 only provides a lower limit on  $N(\rm H\,I)$  of  $10^{17.7}$  cm<sup>-2</sup>. The partial breaks seen towards UVQS J2017–4516 and UVQS J2019–5042 yield  $\log N(\rm H\,I)/\rm cm^{-2} \approx 16.6$  and 16.8, respectively. These  $N(\rm H\,I)$  values are consistent with the ones obtained using single cloud COG analysis.

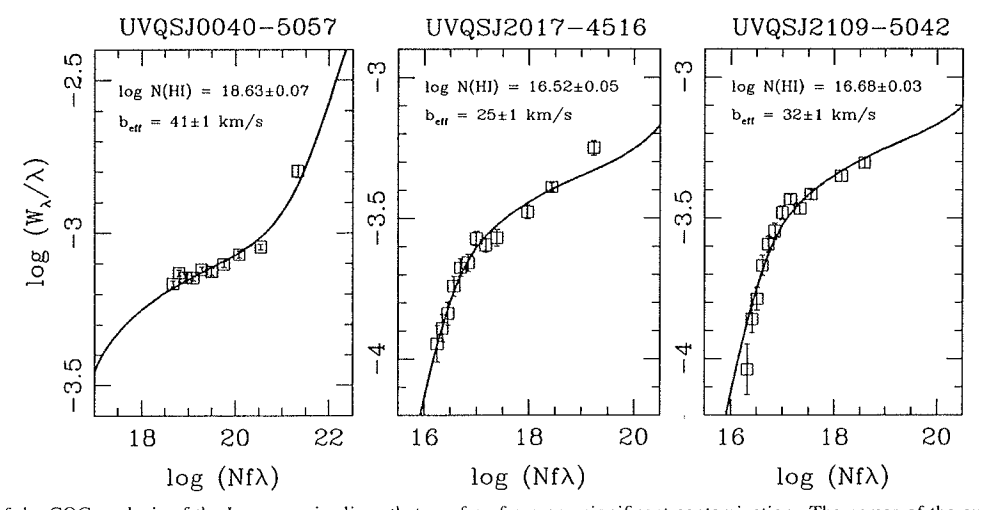


Figure 2. Results of the COG analysis of the Lyman series lines that are free from any significant contamination. The names of the quasars are given in the top. Note that the errors in the equivalent width measurements and hence in the inferred column densities are underestimated since the continuum placement uncertainties are not taken into account. An error of 0.10–0.15 dex in  $\log N(\rm H\,\textsc{i})$  is more reasonable. The Ly $\alpha$  line from the  $z_{\rm abs}=0.43737$  system towards UVQSJ0040–5057 falls on the damping part of the COG. In fact, we do see a weak damping wing in the Ly $\alpha$  absorption.

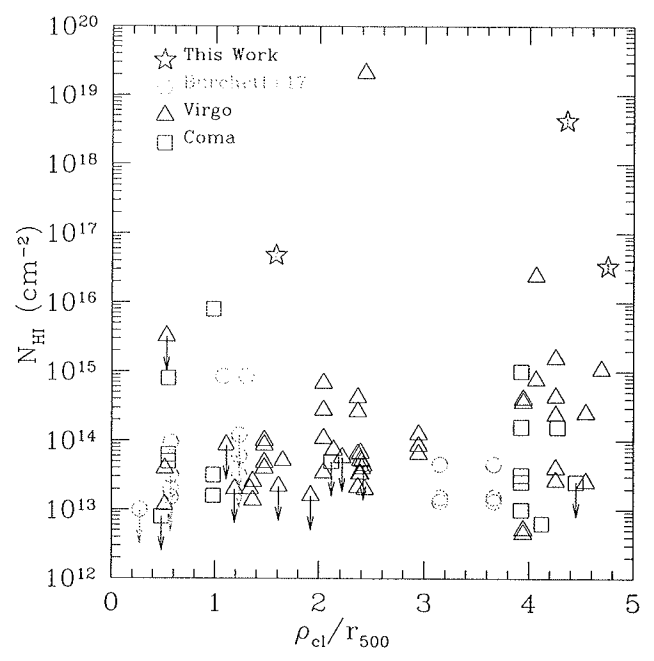


Figure 3. H1 column density against clustocentric impact parameter normalized by  $r_{500}$ . The data points corresponding to the Virgo and Coma clusters are from Yoon et al. (2012) and Yoon & Putman (2017). Since no convincing Ly $\alpha$  absorption is seen within  $\pm 2000$  km s<sup>-1</sup> of the cluster MaxBCG J217.847+24.683 in Burchett et al. (2017), we have assumed  $N({\rm H\,I}) < 10^{13}$  cm<sup>-2</sup> which is consistent with the error spectrum. No obvious trend is seen in the  $N({\rm H\,I})$  radial profile.

Yoon & Putman (2017). We have used the publicly available code massconvert (Hu & Kravtsov 2003), which assumes a NFW density profile, to convert the  $M_{\rm 200}$  values of Coma  $(1.4 \times 10^{15} M_{\odot})$  and Virgo  $(2.2 \times 10^{14} M_{\odot})$  as given in Yoon & Putman (2017) to  $M_{500}$  ( $r_{500}$ ). The impact parameters of the quasar sightlines with respect to Virgo, which are not explicitly given in Yoon et al. (2012), are calculated assuming the center of the cluster to be the center of Cluster-A containing M87. Note that a velocity window of  $\pm 3024$  km s<sup>-1</sup> around the systemic velocity of Coma and a velocity window of -438 to +1862 km s<sup>-1</sup> around the systemic velocity of Virgo were considered by the authors for connecting absorbers to the corresponding cluster. The lower bound in velocity for Virgo was affected by the Galactic Ly $\alpha$  absorption. In Fig. 3 we also compare to the recent study of Burchett et al. (2017) who have presented H I column densities around 7 X-ray detected clusters in the redshift range 0.1-0.45 and within a velocity window of  $\pm 2000 \,\mathrm{km} \,\mathrm{s}^{-1}$ . The massconvert routine is used to convert their  $M_{200}$  values to  $M_{500}$   $(r_{500})$ .

The lack of any trend between  $N({\rm H~I})$  and the normalized clustocentric impact parameter is evident from Fig. 3. This is in contrast to the results of absorption line studies of the CGM (e.g., Prochaska et al. 2011; Tumlinson et al. 2013) in which an anti-correlation between  $N({\rm H~I})$  (or equivalent width) and impact parameter is routinely seen. Next, we note that the SZ-effect selected clusters from this study are the ones that exhibit the highest H I column densities in the outskirts. Only 3.7% (2/54) of the Virgo-sightlines show a partial Lyman limit system (pLLS;  $N({\rm H~I}) > 10^{16.2}~{\rm cm}^{-2}$ ). None of the Comasightlines show a pLLS. Note that, owing to the low redshifts, the  $N({\rm H~I})$  measurements for Virgo and Coma rely only on the Ly $\alpha$  line and the systems with  $N({\rm H~I}) > 10^{14.5}~{\rm cm}^{-2}$  are presumably saturated. Nonetheless, even if we as-

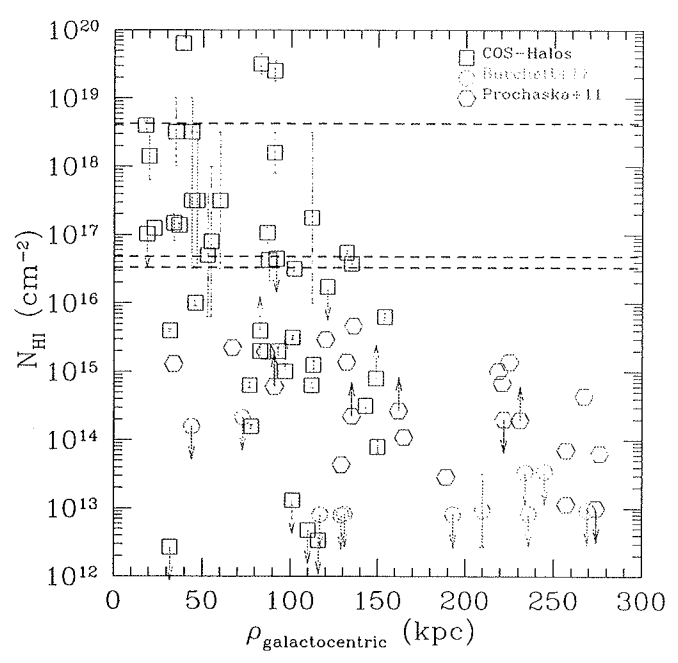


Figure 4. The radial profile of H1 absorbing gas around galaxies. The (blue) squares represent  $L\sim L_*$  field galaxies at  $z\approx 0.2$  studied by the COS-Halos team (Werk et al. 2014; Prochaska et al. 2017). The (magenta) hexagons are from the sample of galaxies with  $L>0.1L_*$  from Prochaska et al. (2011). Note that for each of these galaxies at least one additional galaxy with  $L>0.1L_*$  has been detected within 3 Mpc of the sight line and with  $|\Delta v|<400~{\rm km~s^{-1}}$ . The (orange) circles represent the cluster galaxies from Burchett et al. (2017). The horizontal dashed lines are the  $N({\rm H\,I})$  values for the three clusters studied here.

sume that all of the absorbers with  $N({\rm H\,I})>10^{14.5}~{\rm cm}^{-2}$  towards Virgo and Coma are pLLS, the fraction is only  $\approx 20\pm 5\%~(14/71)$ . None of the absorbers in Burchett et al. (2017) sample are pLLS. The highest  $N({\rm H\,I})$  they observed is  $10^{14.93\pm0.03}~{\rm cm}^{-2}$ , which is well constrained by the presence of Ly $\alpha$ , Ly $\beta$ , and Ly $\gamma$  lines. All other absorbers have log  $N({\rm H\,I})/{\rm cm}^{-2} < 14.1$ . In Section 4, we return to the issue of apparent abundance of strong H I absorbers towards our targeted SZ-clusters.

In Fig. 4 we show the HI column density profile around low-z galaxies using 3 different galaxy samples from the literature. The COS-Halos points represent the N(HI) profile around isolated, bright ( $\sim L_*$ ) galaxies within  $\pm 600~{
m km~s^{-1}}$ . For the sample of Prochaska et al. (2011) we have selected the galaxies with at least one additional  $L > 0.1L_*$  galaxy detected within 3 Mpc of the sightline and with velocity offset  $|\Delta v| < 400$  km s<sup>-1</sup>. Therefore these data points essentially provide the radial profile of N(HI) around group galaxies. Here we note that some of the COS-Halos galaxies might also have companions within 3 Mpc and  $|\Delta v| < 400 \text{ km s}^{-1}$ The points corresponding to Burchett et al. (2017) are for cluster galaxies with  $ho_{
m galactocentric} < 300$  kpc and  $|\Delta v| <$  $600 \text{ km s}^{-1}$ . We note that at any given impact parameter, when data are available, the field galaxies tend to have the highest column densities followed by the group galaxies. As noted by Burchett et al. (2017), a significant suppression in N(HI) is apparent for their cluster galaxies. The N(HI) measurements of the SZ-clusters, as indicated by the dotted lines, are more than two orders of magnitude higher than the measurements/limits obtained by Burchett et al. (2017).

#### 4. DISCUSSION & SUMMARY

The HI column densities we measure (i.e., N(HI) >  $10^{16.5} \text{ cm}^{-2}$ ) in the outskirts ( $\rho_{\rm cl}/r_{500} = 1.6 - 4.7$ ) of SZ-selected clusters are clearly significantly higher than the other existing measurements around X-ray detected clusters (see Fig. 3). One of the possible reasons could be that the strong H I absorbers we detect are not related to the targeted clusters. Recall that we noticed large velocity offsets (i.e., -2600, -2100, and +9000 km s<sup>-1</sup>), albeit consistent within the  $1\sigma$  uncertainties, between the absorber's and the cluster's redshifts. We, therefore, calculate the probability of random occurrence of each absorber around the cluster redshift within the  $\pm 1\sigma$  uncertainties in the photometric redshifts (see

Table 1) by using the observed  $\frac{d\hat{N}(>N,z)}{dz}$  of low-z H1 absorbers (Danforth et al. 2016). The probabilities turn out be < 4.2%, 6.3%, and 8.7% for the absorbers towards J0040-5057, J2017-4516, and J2109-5042 respectively. Since the events are independent, the compound probability of random occurrence of all three absorbers is < 0.02%. Thus it is unlikely that the absorbers are unrelated to the clusters. Nonetheless, spectroscopic confirmation of the redshifts of the clusters is of utmost importance.

One of the interesting questions regarding the nature of the absorbers is: do they arise from the CCM or are they related to the CGM of cluster galaxies close to the lines of sight? If they are related to the CGM of  $\sim L_*$  galaxies as in the COS-Halos survey, then it is evident from Fig. 4 that the hostgalaxies would be detected within 150 kpc of the QSO lines of sight. The majority of the absorbers with metal lines towards Virgo and Coma also have galaxies within 300 kpc and  $300 \text{ km s}^{-1}$  (Yoon & Putman 2013, 2017). Note that, we also detect a range of metal lines (e.g., C11, C111, N111) from all of these absorbers. A faint dwarf galaxy very close to the QSO (possibly within the QSO PSF) can also produce such strong H I absorption. Alternatively, these absorbers could be probing stripped-off CGM material far away from the hostgalaxies. A uniform search for bright continuum-emitting and faint line-emitting galaxies in these fields, using facilities like the VLT/MUSE, is crucial for a better understanding of the origin(s) of the absorbers.

Our single component COG analyses of the Lyman series lines yielded  $b_{\rm eff}$  in the range of 25–41 km s<sup>-1</sup> (Fig. 2). This corresponds to a non-thermal broadening of 21–38 km s -1 assuming the temperature of the H I absorbing gas is  $\sim 10^4$  K. The presence of multiple (unresolved) components and/or higher gas temperature would only lessen the non-thermal contribution to the line broadening. In hydrodynamical simulations, the predicted merger-induced random gas motions are on the order a few 100 km s<sup>-1</sup> in the outskirts of galaxy clusters (see e.g., Fig. 4 in Nagai et al. 2013). The measured  $b_{\rm eff}$ values are consistent with the ones observed in the CGM of individual low-z galaxies (see e.g., Fig. 11 in Tumlinson et al. 2013) but are significantly lower than the values predicted in simulations of cluster outskirts. This suggests that the observed H1 absorbing gas is associated with the collapsed substructures as opposed to the CCM at large.

If the absorbers stem from the CGM of cluster galaxies, then the difference of more than two orders of magnitude in N(HI) compared to the measurements/limits placed by Burchett et al. (2017) is intriguing (see Fig. 4). We note that the clusters in Burchett et al. (2017) are X-ray detected and primarily at  $z \lesssim 0.2$  but with masses ( $\sim \text{ few} \times 10^{14} \ M_{\odot}$ ), by and large, similar to our SZ-selected clusters at  $z \approx 0.46$ .

It is unlikely that the redshift difference could make such a drastic difference in the observed N(H1) values. We further note that no unambiguous HI absorption is detected (e.g., N(HI) <  $10^{14.3}$  cm<sup>-2</sup>) from the highest redshift cluster galaxy ( $z_{\rm gal}$  =0.4560) towards the cluster GM-BCG J255.55+64.23 in the sample of Burchett et al. (2017). This supports the idea that redshift evolution of cluster outskirts is unlikely to be the cause. However, currently we are restricted by a very small sample. UV spectroscopic observations of many more galaxy clusters are indispensable for further advancement.

Yoon et al. (2012) have noticed that the sightlines passing through substructures in the periphery of Virgo are likely to have higher Ly $\alpha$  equivalent widths. The same scenario might be true for the systems studied here. In fact, a detection of a metal-poor ([O/H] = -1.6), sub-damped Ly $\alpha$ absorber (sub-DLA;  $\log N({\rm H\,I})/{\rm cm}^{-2} \approx 19.3$ ) has been reported by Tripp et al. (2005) in the outskirts of Virgo near the NGC 4261 galaxy group (see Fig. 3). Interestingly, no bright galaxy with a small impact parameter has been found by the authors. The nearest known sub- $L_*$  and  $L_*$  galaxies have impact parameters of  $\approx 90$  kpc and  $\approx 260$  kpc respectively. From the observed low metallicity, the underabundance of nitrogen, and the lack of  $\alpha$ -element enhancement the authors argued that the absorber is related to a dwarf galaxy and/or a high velocity cloud in the outskirts of Virgo. The strongest absorber in the sample of Burchett et al. (2017), with  $\log N({\rm H\,I})/{\rm cm}^{-2} \approx 14.9$ , also does not have any bright galaxy counterpart within 300 kpc and  $|\Delta v| < 400 \text{ km s}^{-1}$ . In this case, the sightline passes through the interface of subclusters A1095W and A1095E. The authors have suggested that stripping from a far away galaxy or a density enhancement due to a merger shockwave are possible origins for the cool gas detected in absorption.

In addition to strong HI, all three systems exhibit strong absorption lines from low- (e.g., C II $\lambda$ 1036) and intermediate-(e.g., C IIIλ977, N IIIλ989) ionization metal lines, suggesting high metallicity gas. Weak high-ionization lines (e.g., O VI, Ne VIII) might also be present in at least one of them. A detailed analysis of the metal lines, along with ionization models, will be presented in future papers. The analysis of the detected metal lines will provide further insights into the nature of the absorbers.

Support for this research was provided by NASA through grants HST GO-14655 from the Space Telescope Science Institute, which is operated by the Association of Universities for Research in Astronomy, Inc., under NASA contract NAS5-26555. SM and JS acknowledge support from European Research Council (ERC), Grant Agreement 278594-GasAroundGalaxies.

#### REFERENCES

Bahé, Y. M., Barnes, D. J., Dalla Vecchia, C., et al. 2017, ArXiv e-prints, arXiv:1703.10610

Bleem, L. E., Stalder, B., de Haan, T., et al. 2015, ApJS, 216, 27 Burchett, J. N., Tripp, T. M., Wang, Q. D., et al. 2017, ArXiv e-prints, arXiv:1705.05892

Danforth, C. W., Stocke, J. T., & Shull, J. M. 2010, ApJ, 710, 613 Danforth, C. W., Keeney, B. A., Tilton, E. M., et al. 2016, ApJ, 817, 111 Gonzalez, A. H., Sivanandam, S., Zabludoff, A. I., & Zaritsky, D. 2013,

Gonzalez, A. H., Zaritsky, D., & Zabludoff, A. I. 2007, ApJ, 666, 147 Green, J. C., Froning, C. S., Osterman, S., et al. 2012, ApJ, 744, 60

Xray vs SZ-selected

- Hu, W., & Kravtsov, A. V. 2003, ApJ, 584, 702
- Kacprzak, G. G., Muzahid, S., Churchill, C. W., Nielsen, N. M., & Charlton, J. C. 2015, ApJ, 815, 22
- Lau, E. T., Nagai, D., Avestruz, C., Nelson, K., & Vikhlinin, A. 2015, ApJ, 806, 68
- Monroe, T. R., Prochaska, J. X., Tejos, N., et al. 2016, AJ, 152, 25 Nagai, D., Lau, E. T., Avestruz, C., Nelson, K., & Rudd, D. H. 2013, ApJ,
- Osterman, S., Green, J., Froning, C., et al. 2011, Ap&SS, 335, 257 Prochaska, J. X., Weiner, B., Chen, H.-W., Mulchaey, J., & Cooksey, K. 2011, ApJ, 740, 91
- Prochaska, J. X., Werk, J. K., Worseck, G., et al. 2017, ApJ, 837, 169 Simionescu, A., Allen, S. W., Mantz, A., et al. 2011, Science, 331, 1576 Tripp, T. M., Jenkins, E. B., Bowen, D. V., et al. 2005, ApJ, 619, 714
- Tumlinson, J., Thom, C., Werk, J. K., et al. 2013, ApJ, 777, 59 Turner, M. L., Schaye, J., Steidel, C. C., Rudie, G. C., & Strom, A. L. 2014,
- MNRAS, 445, 794 Urban, O., Simionescu, A., Werner, N., et al. 2014, MNRAS, 437, 3939
- Voit, G. M. 2005, Reviews of Modern Physics, 77, 207
- Walker, S. A., Fabian, A. C., Sanders, J. S., & George, M. R. 2012, MNRAS, 427, L45
- Werk, J. K., Prochaska, J. X., Tumlinson, J., et al. 2014, ApJ, 792, 8 Yoon, J. H., & Putman, M. E. 2013, ApJ, 772, L29
- --. 2017, ApJ, 839, 117
- Yoon, J. H., Putman, M. E., Thom, C., Chen, H.-W., & Bryan, G. L. 2012, ApJ, 754, 84

2b) 
$$\lambda_{rest} = 912$$
  $Z = 0.51484 \approx 0.515$   
 $\lambda_{obs} = \lambda_{rest} (1+Z)$   
 $\lambda_{obs} = 912 (1+0.515) = 1381.7 \text{ Å} (or 1381.534 Å)$ 

Ze) 
$$F = F^{c} \exp(-\tau)$$
  $\longrightarrow \chi = \ln\left(\frac{F^{c}}{F}\right) = \chi = \ln\left(\frac{F^{c}}{F}\right)$ 

From Fig 1 blue deshed line F = 2.3 × 10-15 From Fig 1 red solid line F = 1.5×10-15  $\frac{F^{c}}{F} = \frac{7.3}{1.5} = 1.53$   $\rightarrow 2 \left(1.53\right) = 2 = 0.42$ 

from 
$$7 = N\sigma \rightarrow N = \frac{7}{\sigma} = \frac{0.42}{6.03 \times 10^{-18}} = 7.08 \times 10^{-16}$$

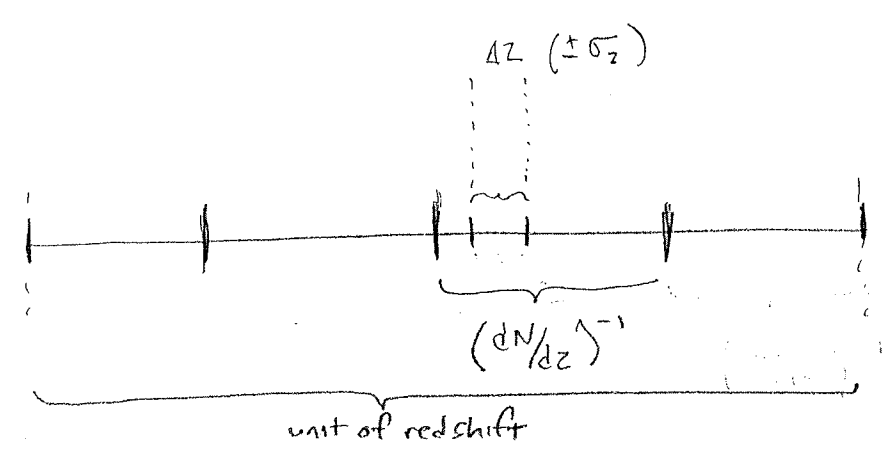
$$\log N = 16.85$$
author's grote 16.8!

3c.) We want absorbers with 
$$N>10^{15}$$
 cm. These are (from Table I of exam). With  $\Delta Z=2.3-0.6=1.7$ 

$$5000-123 \ Z=2.170 \ log N=15.80$$

$$J000-123$$
  $z=2.170$   $log N=15.80$   
 $J0345+051$   $z=2.209$   $log N=17.90$   $N=4$   $dN=4$   
 $J1038+459$   $Z=1.836$   $log N=16.38$   
 $J2022-001$   $z=0.750$   $log N=19.03$ 

4e.)



This example is for dN/dz = 4 in which case, the redshift that is a string to affind that absorber in would be  $(dN/dz)^{-1} = \frac{1}{4}$  of a unit redshift.

So to find an absorber in range AZ you would have the chance  $\frac{4Z}{\left(\frac{dN}{dz}\right)^{-1}} = P$ 

 $\frac{\Delta Z}{1+Z} = \frac{\Delta V}{C} \qquad \Delta V = 9000 \text{ Km/s}$ 

4b)  $\frac{dZ}{1+Z} = 9000 \text{ km/s} = 0.03$  and Z = 0.51484This is given in paper, or you can derive it from

 $\delta \Delta Z = 0.03 (1+Z)$ 

AZ= 0.03(1.515)

ΔZ = 0.045

$$\frac{dN}{dz} = 16(1+z)^{2.3} \left(\frac{N}{10^{14}}\right)$$

$$Z = 0.515$$

$$N = 10^{16.68}$$

$$S = 0.515$$

42)

$$\Delta Z = 0.045$$
 ±6 means total  $\Delta Z = 2(0.045) = 0.09$ 

$$P = \frac{\Delta^{2}}{(dN/dz)^{-1}} = \frac{0.09}{1.03} = 0.087 \Rightarrow \sqrt{8.7\%}$$
spot on!

		: · · ·
		,